SHEAR DEFORMATION OF AMORPHOUS AND NANOCRYSTALLINE COPPER MICROSTRUCTURES VIA ATOMISTIC SIMULATION

by

David R. Gandy

SUBMITTED TO THE DEPARTMENT OF MECHANICAL ENGINEERING
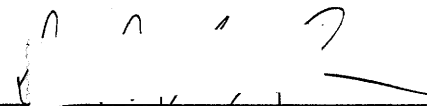IN PARTIAL FULFILLMET OF THE REQUIREMENTS FOR THE DEGREE OF

BACHELOR OF SCIENCE IN MECHANICAL ENGINEERING
AT THE
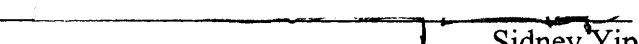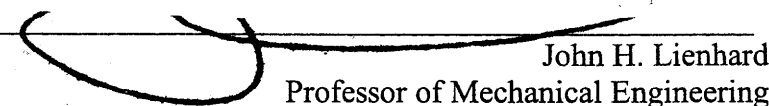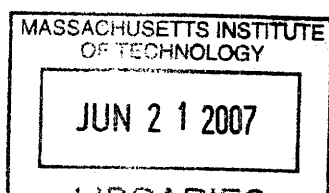MASSACHUSETTS INSTITUTE OF TECHNOLOGY

JUNE 2007

Signature of Author_____
Department of Mechanical Engineering
May 11, 2007

Certified by_____
Sidney Yip
Professor of Nuclear Science and Engineering
Thesis Supervisor

Accepted by_____
John H. Lienhard
Professor of Mechanical Engineering
Chairman, Undergraduate Thesis Committee

1

SHEAR DEFORMATION OF AMORPHOUS AND NANOCRYSTALLINE COPPER MICROSTRUCTURES VIA ATOMISTIC SIMULATION

by

David R. Gandy

ABSTRACT

In the well-known Hall-Petch behavior, yield and flow stresses in polycrystalline metals increase with a decrease in grain size. As grain size continues to decrease, mechanical strength peaks. As grain size further decreases, mechanical strength begins to decrease. As grain size approaches zero, the total structure is composed of an increasingly high percentage of grain boundaries, which exhibit the properties of an amorphous structure. Molecular dynamics simulations, with the goal of exploring this behavior, were performed on nanocrystalline and amorphous microstructures using the embedded atom potential developed by Mishin et al. A 0.2 shear strain was applied to each of the nanocrystalline and amorphous samples. From these simulations, we have observed the inverse Hall-Petch behavior of nanocrystalline structures. We have also shown that the amorphous structure as zero grain size is reasonable as the limiting case for the inverse Hall-Petch trends in nanocrystalline structures

ACKNOWLEDGEMENTS

In honesty, there is no way to express the extent of my gratitude for help that has been provided by Robert Boyer for the numerous hours he has spent with me in the realization of this thesis. As he is a tremendously gifted and natural teacher, I hope that he continues to exercise this talent in the years to come. Without his help, this thesis would never exist.

I would like to thank Professor Yip for his advising and providing this excellent opportunity. My undergraduate career has been enriched as a result.

I would also like to thank Jennifer Whiteside for her love and support during the final stages of my time at MIT. Things in my life seem to be happening all at once right now, and I'm thankful that she is the best part. I could not ask for a better best friend.

I would like to thank my friends and all the people who encouraged me over the years to complete my undergraduate degree. Particularly to Holly Hair for a life shifting conversation at a hotel in Beijing. This thesis is the fruit of all of those encouragements.

Lastly, I would like to thank my parents. They never pushed me to go to MIT, nor did they push me to return. They just told me I should do what I Knew to be right. As long as I continue to do so, I will always be in exactly the right place.

TABLE OF CONTENTS

1 INTRODUCTION

Nanocrystalline metals have received increasing attention since the 1980s, in part due to their desirable strength [1]. This has caused the relationship between nanocrystalline grain size and mechanical performance to become an important focus of study in the field of nanocrystalline materials [2]. Previous study in the field has discovered a phenomenon where as grain size decreases, mechanical strength increases, known as Hall-Petch behavior [3]. Furthermore, as grain size decreases, mechanical strength peaks, and then begins to decrease as grain size decreases further. This final regime is known as the inverse Hall-Petch. Nanocrystalline metals have been extensively studied over the last decade, however a complete set of deformation mechanisms governing yield strength remains somewhat unclear [4].

An important tool in our study of these nanocrystalline mechanical properties is the use of molecular dynamics (MD) simulation. A key advantage of MD simulation is the ability to investigate, in situ, atomistic mechanisms more closely than is allowed in a laboratory setting. As computing environments grow exponentially more powerful, our ability to simulate nanocrystalline materials also grows. More powerful computers of increased speed and memory allow us to perform more complicated simulations with some combination of increased duration and larger system size.

Shear strain of nanocrystalline microstructures is fundamental to understanding the onset of plasticity and eventual failure. Our atomistic simulations will investigate the behavior of shear strain for polycrystalline copper in the inverse Hall-Petch regime using embedded atom potentials developed by Mishin et al [5]. Amorphous and nanocrystalline samples of varying grain sizes will be subjected to a strain of 0.2 at a strain rate of 10^9 s^{-1}. As grain size decreases, a larger percentage of total volume is made up of grain boundaries. We propose that the amorphous sample can be approximated as zero grain size and can be considered the limiting case for inverse Hall-Petch behavior.

2   BACKGROUND

2.1   *Atomistic Molecular Dynamics Simulation*

An advantage to atomistic simulation comes in the ability to track, in situ, local atomic behavior. Molecular dynamics (MD) simulation attempts to replicate individual atomic interactions and behavior based on properties that are governed by quantum mechanics and determined from experimental data [6]. For each atom, simulation begins by calculating which other atoms are in an interaction radius, commonly known as the "neighbor list" [6]. Using the neighbor list, energies and forces are then calculated based on an energetic potential, which is discussed in more depth in next section. In order to allow simulation of atomic vibration, the time step between each iteration must be in the realm of femtoseconds (10^{-15}). It is obvious that for a simulation of any reasonable size that the simulation process is tremendously intensive computationally. As the number of particles in a system begins to range in the millions, choosing computational methodologies and algorithms is of vital importance.

Additional advantages of MD simulation also exist. It allows us to perform experiments in a perfectly controlled environment, free of contamination. A single prepared sample can be reused for an infinite number of experiments. It also allows us to perform experiments employing just a single computer, without the need for extensive and expensive laboratory equipment. However, these advantages only truly exist when the atomistic simulation method is acceptably accurate as compared to a laboratory counterpart.

2.2 Empirical Potentials: The Embedded-Atom Method

The obvious question raised by performing atomistic simulation, as compared to laboratory experimentation, is how accurately these simulations can model the physical world. Our ability to model complex atomistic structures is limited by our understanding of their physical properties. Experiments can now resolve the atomic-scale structure of grains and grain boundaries [7].

The pair potential model tells us that the total energy of a system is the sum of energy potential between each pair of atoms [7]:

$$E = \frac{1}{2} \sum_{i \neq j} V(r_{ij}) \tag{2.1}$$

where each atomic pair contributes $V(r_{ij})$, where r_{ij} is the distance between atoms i and j. The function $V(r_{ij})$ is experimentally determined for the material of interest.

The pair potential method considers each atomic bond independent of all others. This is particularly erroneous for metals, where the bonding resulting from the many-body effect, often described as a "sea of valence electrons" [8], remains unconsidered. Therefore, the pair potential model lacks a fundamental component of the total system energy, which makes it less useful as a reliable equation to govern simulation.

The past 25 years have seen an improvement over the pair potential model with the development of the embedded-atom method (EAM) [7]. The EAM provides an approximation of the many-body effects neglected by the pair potential. The EAM potentials are given by the equation:

$$E = \sum_i G_i \left(\sum_{j \neq i} \rho_j (r_{ij}) \right) + \frac{1}{2} \sum_{i \neq j} V(r_{ij}) \tag{2.2}$$

where G_i is the embedding energy, ρ_j is the electron density from the sum of neighboring atoms, and $V(r_{ij})$ is the energy from two-atom interactions.

For a wide range of metallic systems to be modeled by the EAM, physically meaningful potentials have been developed using various fitting schemes for the general form of equation 2.2. As compared to the pair potential, the additional term contained in the EAM allows it to be particularly accurate for the modeling of metallic bonding. In the case of homogenous copper, EAM potentials developed by Mishin et al [9] are particularly desirable [10]. We will use this model developed my Mishin et al for our simulation of nanocrystalline and amorphous copper microstructures.

2.3 Normal and Inverse Hall-Petch Behavior

The strength of polycrystalline metals increases with a decrease in grain size, a phenomenon known as on the Hall-Petch relationship. For coarse grains larger than ~100 nm, the effect of grain diameter on yield stress is given by the empirical Hall-Petch relationship [7]:

$$\sigma_y = \sigma_0 + Kd^{-1/2} \tag{2.3}$$

where σ_y is the yield stress, σ_0 is the friction stress, K is the Hall-Petch slope, and d is the grain size. This relationship suggests that as grain size decreases yield strength increases and has been shown accurate for a wide variety of materials.

The effect of grain size on yield strength becomes more complicated as diameters decrease to ~100 nm. For grain sizes between ~100 nm and ~10 nm, the Hall-Petch slope K remains positive, but is decreased in value. At a grain size of ~10 nm, the mechanical strength peaks. Then, as grain size continues to decrease, strength begins to decrease. This final regime is known as inverse Hall-Petch [11]. Figure 2-1 shows a generic representation of normal and inverse Hall-Petch yield strength behaviors.
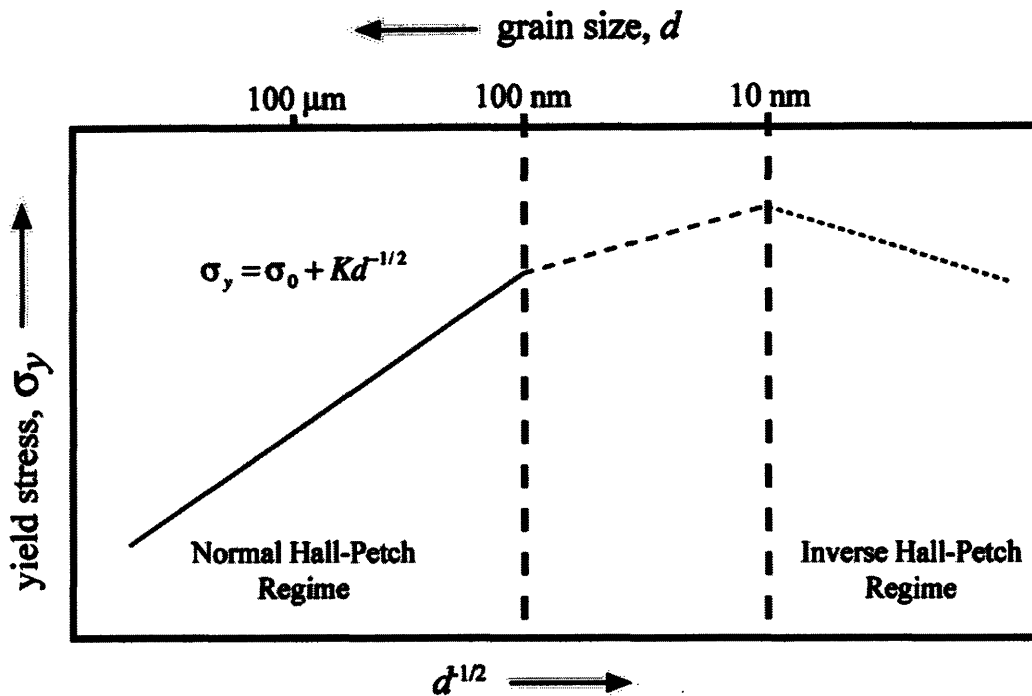

Figure 2-1: Generic representation of normal and inverse Hall-Petch yield strength behavior.

Atomistic simulations by Schiotz et al revealed that for nanocrystalline copper with grain sizes ranging between 5 to 50 nm, yield stress crossover from normal to inverse Hall-Petch occurred at a grain diameter of ~14 nm [12]. As all of our nanocrystalline samples will be sufficiently below 14 nm in grain diameter, the yield stress and grain size relationship for our simulations will remain in the inverse Hall-Petch regime.

3 PROCEDURE

3.1 Introduction

Our procedure begins with the preparation of nanocrystalline and amorphous samples, which will eventually be subjected to a shear strain of up to 0.2. For our nanocrystalline samples, this process starts by geometrically generating a structure of 16 randomly oriented body centered cubic (BCC) grains, of which each grain is made up of perfect face centered cubic (FCC) copper. This process is repeated for the creation of our amorphous sample with one difference. Instead of 16 grains, we create a structure of a large enough number of grains that the sample no longer has recognizable grains. As constructed, all nanocrystalline and amorphous samples must then be relaxed such that the residual stresses along the principle axes are brought to a negligible level. After this relaxation has been performed, our nanocrystalline and amorphous samples are then be subjected to a shear strain up to 0.2 with a strain rate of 10^9 s^{-1} at a constant 10 K. The desired 0.2 shear strain is obtained over 200,000 time steps, each lasting a femtosecond.

3.2 Initial Nanocrystalline Sample Preparation

For the initial construction of a nanocrystalline sample, we begin by generating a base configuration of perfect FCC crystal. Grain centers are calculated of a 16-grain, BCC superlattice of edge length equal to the base configuration. These grain centers are then associated with a random rotation matrix. A copy of the base configuration is rotated about each grain center according to the rotation matrix. To create each grain, the rotated base configuration is then cut according to its Voronoi polygon [13], which in the case of our BCC lattice is a truncated octahedron. Finally, the grains are assembled to form a polycrystalline sample and any atoms too close to one another are removed. This process is repeated for our four sample edge lengths of 5.06, 7.59, 10.12, and 12.65 nm. Figure 3-1 displays a comparison of the base configuration FCC crystal alongside the BCC superlattice for our 7.59 nm edge length sample. From this figure, it appears reasonable to approximate grain size as one half the edge length.
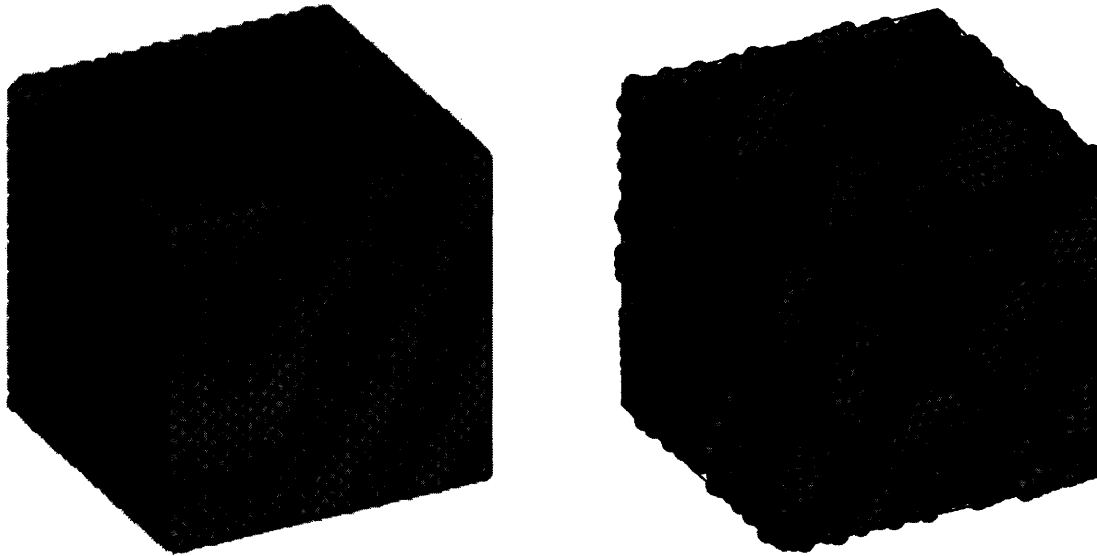

Figure 3-1: Perfect FCC copper crystal (left) is used as the base configuration for generation of a BCC superlattice with 16 grains (right). The polycrystal shown has an edge length of 7.59 nm (particles shaded by coordination number).

3.3 Initial Amorphous Sample Preparation

As grain diameter decreases in size, grain boundaries constitute a larger percentage of the total structure. For small enough grain diameter, the structure is in essence composed entirely of grain boundary, having no recognizable nanocrystalline structure. In order to create an amorphous sample, we perform the same procedure described in the previous section with one change. A sufficiently large enough number of grains are used such that the generated sample is entirely composed of grain boundaries. For a base configuration with an edge length of 7.59 nm, a grain diameter of 0.5 nm creates an effectively amorphous sample. Figure 3-2 shows the result of this process.
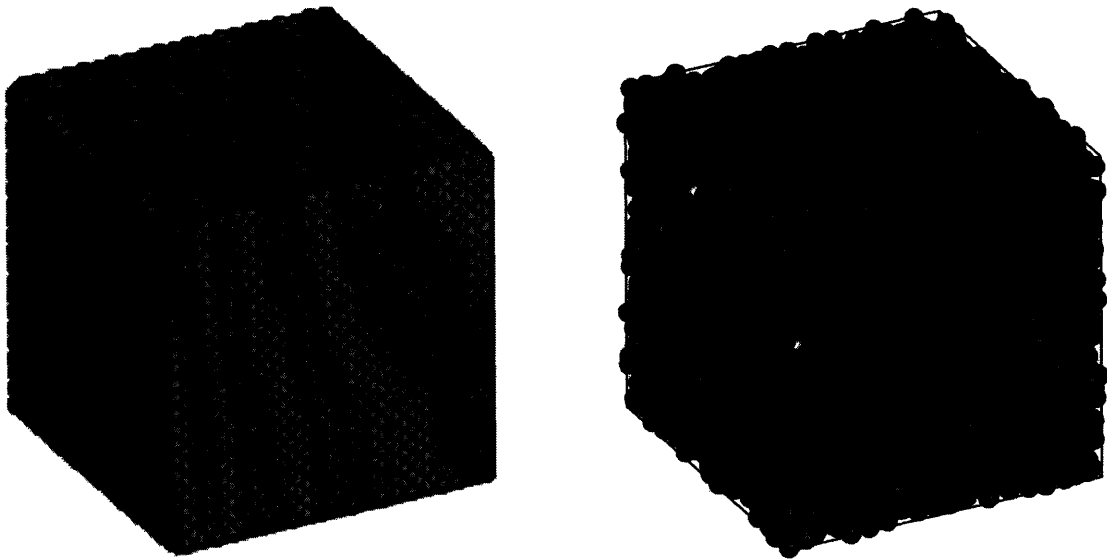

Figure 3-2: Perfect FCC copper crystal (left) is used as the base configuration for the generation of a sample composed in essence entirely of grain boundary (right). The FCC base configuration is the same as is used in the generation of the 7.59 nm edge length nanocrystal (particles shaded by coordination number).

12

3.4 Relaxation Process of Initial Nanocrystalline and Amorphous Samples

As constructed, our samples are not yet ready for our final shear strain simulation. The samples generated by the procedures in the previous sections are geometric creations, having not yet been relaxed. For all nanocrystalline and amorphous samples, we perform an MD run with no input strain at a temperature of 10 K. This allows atoms to locally reorganize themselves according to the accepted computational model developed by Mishin et al. As expected, relaxations show our samples containing non-negligible residual stresses in the principle directions. This behavior is shown in Figure 3-3. Before we can perform a shear deformation, these residual stresses must be minimized to a negligible level.

This requires us to use a process to lower these residual stresses to a point where they can be considered negligible [14]. We perform multiple simulations at a temperature of 10 K for each nanocrystalline and amorphous sample. For each simulation, sample edge length is varied by a small percentage. Figure 3-3 shows a graph of stress versus time for a series of simulations for our 5.0 nm grain diameter sample. During the initial time steps, Figure 3-3 shows a sharp change in principle stress. Over time, grain boundaries reorganize, and the principle stress comes to a steady state.

Residual stresses along the principle directions are then averaged and graphed versus edge length. Figure 3-4 shows the best-fit line used to determine the edge length where the average stress should be minimized. The simulation is again performed to ensure a minimum acceptable internal principle stress has been achieved, generally less than 40 MPa. The final relaxation series in Figure 3-3 shows the relaxation process of the 5.0 nm grain diameter microstructure as it comes to a negligible principle stress level.
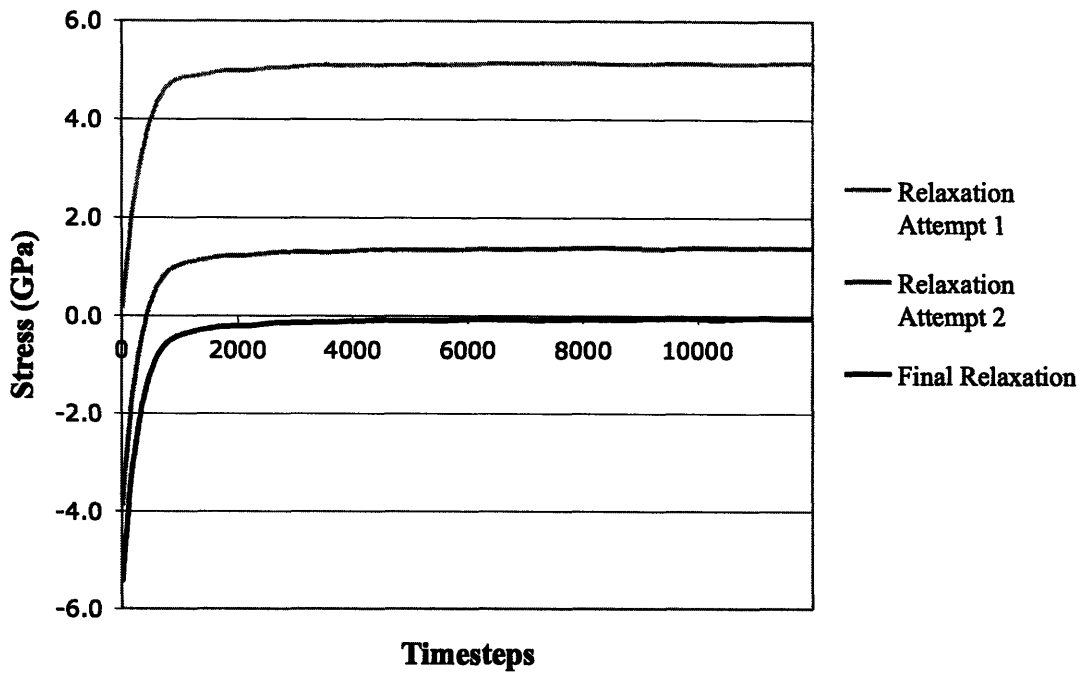
13

Figure 3-3: Stress versus time graph for a series of MD simulations where edge lengths are varied for the 5.0 nm grain diameter sample with no input strain at 10 K.
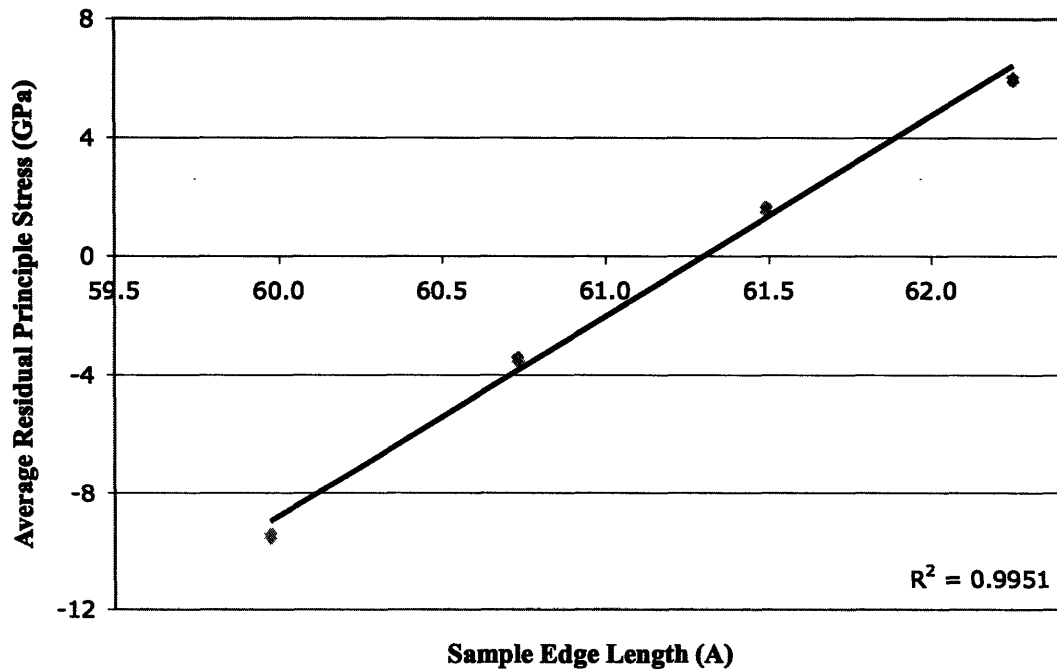

Figure 3-4: Best fit line for average residual principle stress versus sample edge length for 3.7 nm grain diameter nanocrystalline sample.

Relaxation of grain boundaries has resulted in their reorganization. Figure 3-5 illustrates the 10.12 nm edge length polycrystal before and after the relaxation process. While grain boundaries have shifted during relaxation, it appears that the grain diameters still remain approximately one half of the total edge length.
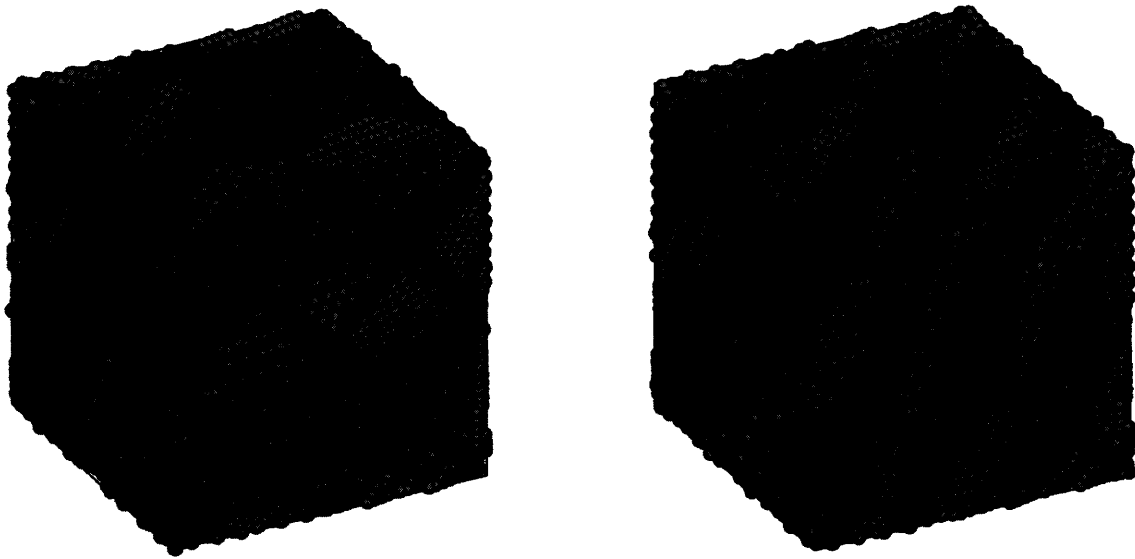

Figure 3-5: Isometric views of 10.12 nm edge length polycrystal before (left) and after (right) the relaxation process (particles shaded by coordination number).

The relaxation process was repeated for all nanocrystalline and amorphous samples, bringing their residual stress levels to a negligible level. Based on the BCC grain arrangement, grain diameters are approximated as one half the relaxed sample edge length. Table 3-1 shows these approximated grain diameters as well as the total particles and edge length for the base configuration and the relaxed microstructure. The amorphous sample has been approximated as a zero diameter grain size.

Table 3-1: A summary of our nanocrystalline and amorphous samples and their characteristics

Sample ID	2.4	3.7	5.0	6.2	Amorphous
Base configuration total particles	10,976	37,044	87,808	171,500	37,044
Base configuration edge length (nm)	5.06	7.59	10.12	12.65	7.59
Relaxed sample total particles	9,565	33,741	81,867	162,137	18,933
Relaxed sample edge length (nm)	4.86	7.40	9.93	12.47	6.12
Relaxed sample grain diameter (nm)	2.4	3.7	5.0	6.2	0

3.5 Shear Deformation of Relaxed Nanocrystalline and Amorphous Samples

Now that the samples have been properly relaxed to negligible principle stresses, we can perform the shear strain simulations that are our primary interest. The relaxed nanocrystalline and amorphous samples are subjected to at a strain rate of 10^9 s^{-1} with a total strain of to 0.2 at a constant 10 K. To achieve the 0.2 strain, the simulation was performed over 200,000 time steps, each lasting a femtosecond (10^{-15}). This allows us to maintain a realistic simulation, as the time step is short enough to model atomic vibration. Figure 3-6 shows us isometric views of a relaxed 5.0 nm grain diameter nanocrystal before and after a 0.2 shear strain.
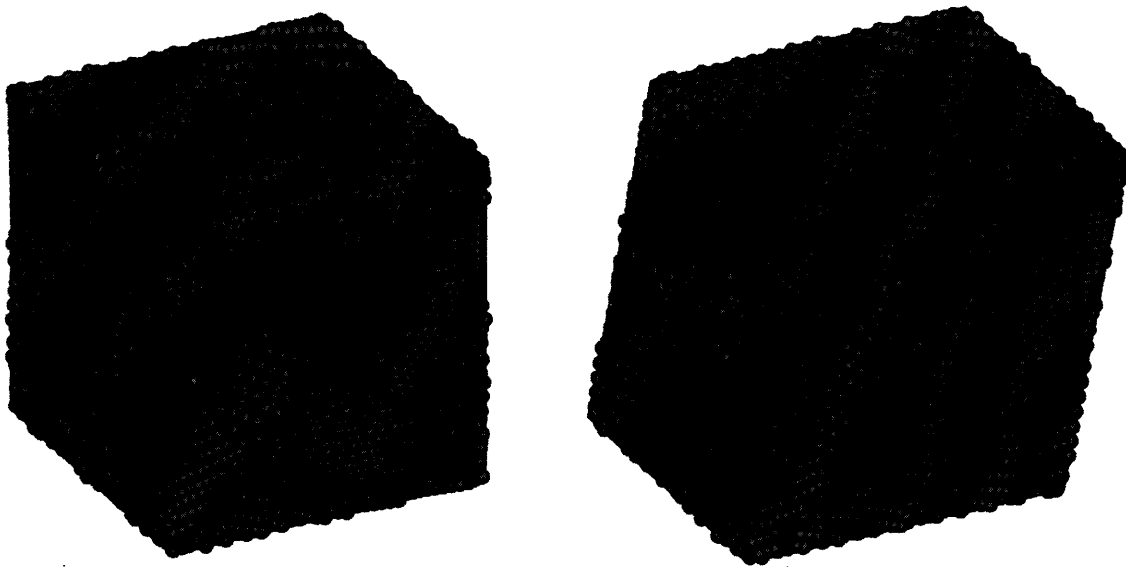

Figure 3-6: Isometric views of relaxed 5.0 nm grain diameter samples before (left) and after (right) 0.2 shear strain (particles shaded by coordination number).

4 RESULTS AND DISCUSSION

4.1 Shear Deformation Yield and Flow Stresses

The principal result of our computations is the stress-strain ($\sigma - \varepsilon$) behavior as obtained from the shear strain simulation of our amorphous and nanocrystalline copper samples. As yield and flow stresses can be difficult to quantify, we first define them according to an established practice for the general case of an ideal $\sigma - \varepsilon$ curve. To determine the yield stress, σ_y, the $\sigma - \varepsilon$ curve is intersected with a line of 0.2% offset ε and a slope calculated as σ/ε for the elastic regime. This intersection is defined as σ_y. The flow stress σ_f is defined as the average stress after the peak has been reached [14]. Figure 4-1 illustrates how σ_y and σ_f are defined.
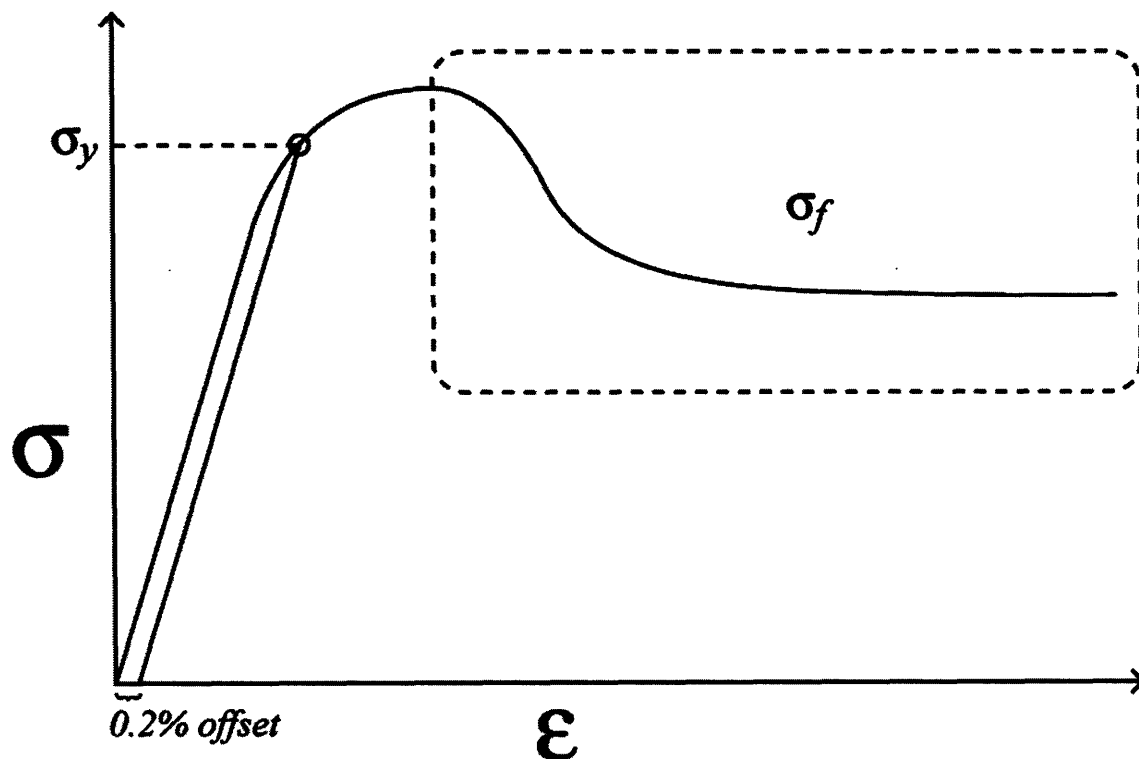

Figure 4-2: Ideal $\sigma - \varepsilon$ curve, showing σ_y at 0.2% offset and σ_f as the average stress after peak.

Multiple curves are shown in Figure 4-2 for grain sizes of 2.4, 3.7, 5.0, and 6.2 nm, as well as our proposed limiting case amorphous sample. Stress versus strain is graphed over a 0.1 shear strain. As grain size decreases, yield and flow stresses also decrease. This is consistent for the expected "inverse Hall-Petch" regime [14]. As approximated as a zero grain diameter, the sheared amorphous microstructure falls below the 2.4 nm diameter sample as expected.
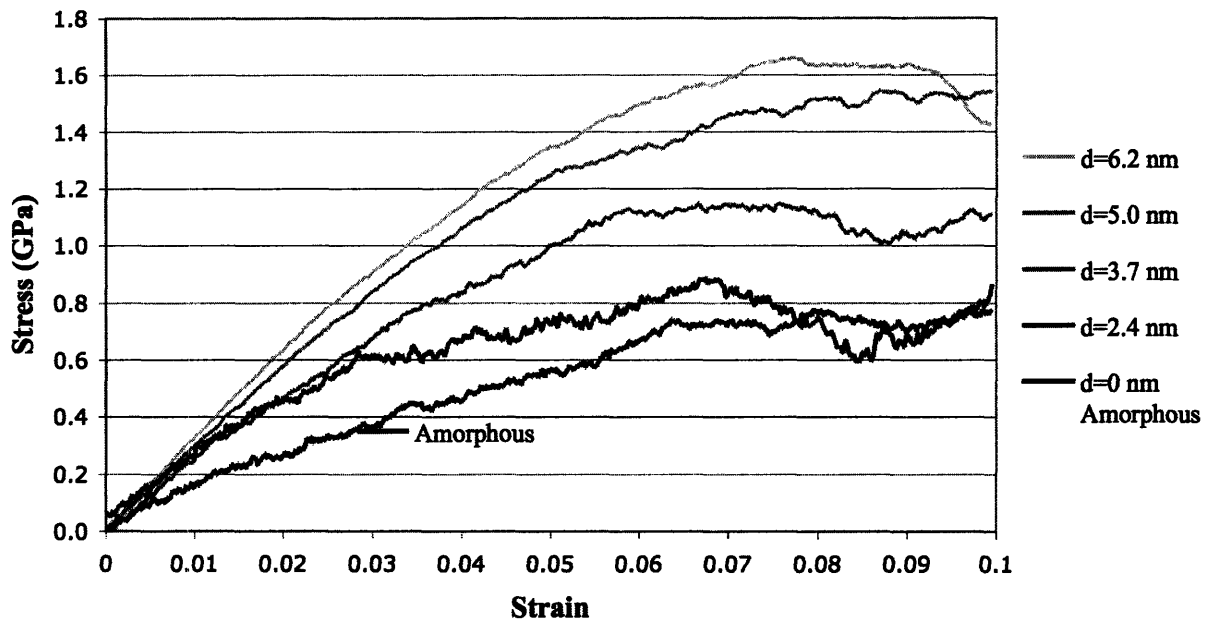

Figure 4-2: $\sigma - \varepsilon$ curves for 0.1 shear strain of samples with nanocrystalline grain sizes ranging from 2.4 to 6.2 nm as well as limiting case amorphous sample, approximated as a zero grain diameter.

From the $\sigma - \varepsilon$ curves found in figure 4-2, yield and flow stresses are calculated from the definitions at the beginning of this section. These results are graphed as a function of grain diameter d, as shown in Figure 4-3, where the amorphous sample is again approximated as a grain diameter of zero. This graph is the principle result of our research.
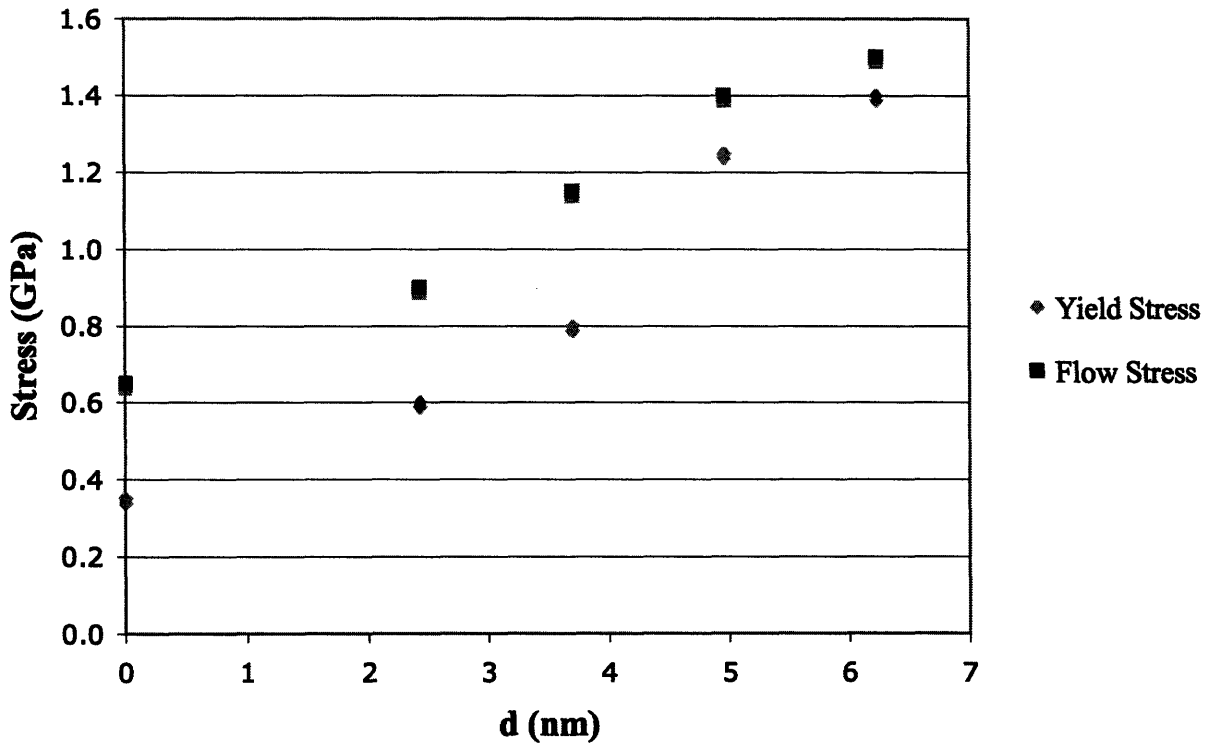

Figure 4-3: Summary of yield stress and flow stresses as a function of grain size for samples of nanocrystalline copper ranging from 2.4 to 6.2 nm. The amorphous sample is approximated as a grain size of zero.

As grain diameter decreases, yield and flow stresses also decrease. This is consistent with the expected inverse Hall-Petch for nanocrystalline grains of this size. Additionally, the yield and flow stress for the amorphous microstructure also clearly fit in to the inverse Hall-Petch trend of the nanocrystalline samples.

4.2 Stress Strain Transition Between Nanocrystalline and Amorphous Copper

Further $\sigma - \varepsilon$ curves for a shear strain up to 0.2 were investigated. Figure 4-3 shows $\sigma - \varepsilon$ curves for grain sizes of 2.4 and 5.0 nm. The $\sigma - \varepsilon$ curves for both of these grain sizes are interesting. The $\sigma - \varepsilon$ curve of the 5.0 nm grain diameter sample is representative of the $\sigma - \varepsilon$ curves for grain sizes larger than 2.4 nm. The curve shows yield stress at a strain of ~0.05, some maximum stress at ~0.08, then plastic flow at a lower value than the maximum stress.

The $\sigma - \varepsilon$ curve for the 2.4 nm grain size sample is also interesting. It shows characteristics similar to those of larger nanocrystalline grain sizes, but also shows characteristics similar to the amorphous sample. For the larger nanocrystalline grain sizes, there is one large difference. When the stress reaches the first peak at ~0.07, it is not the stress maximum for the remainder of the system. Additional stress peaks, each successively higher, are shown at a strain of ~0.13 and ~0.16. Figure 4-3 shows this behavior.
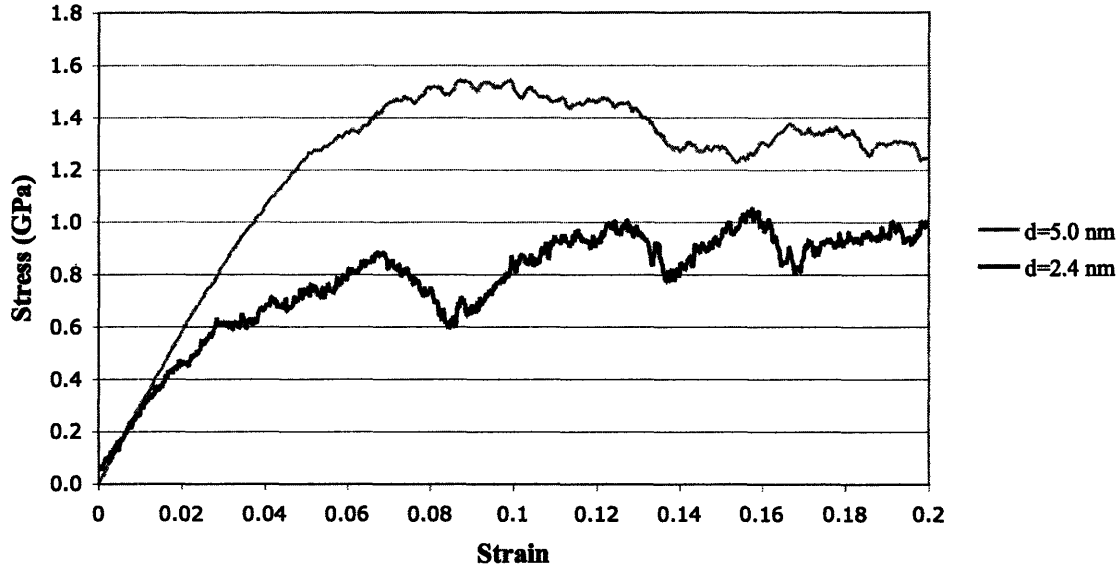

Figure 4-3: Stress-strain curves for 0.2 shear strain of samples with nanocrystalline grain sizes of 5.0 and 2.4 nm.

To further investigate, we have visually inspected the 2.4 nm grain diameter microstructures to determine the dominant mechanism. Figure 4-4 shows the 2.4 nm grain diameter sample before and after a 0.2 shear strain.
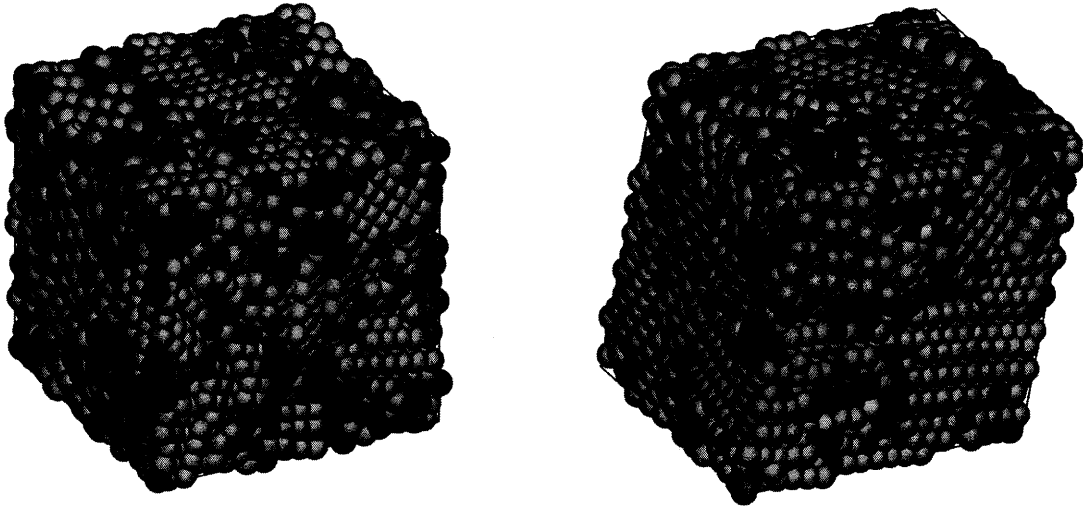

Figure 4-4: Relaxed 2.4 nm grain diameter sample before (left) and after (right) a 0.2 shear deformation.

The first thing that is noticed is that the pre-shear sample appears not to have a definite nanocrystalline grain structure. During relaxation, grain boundaries have shifted to the point that the sample structure appears somewhere between nanocrystalline and amorphous.

As we inspect the 0.2 shear deformation sample on the right of Figure 4-4, we see that a larger percentage of the particles have shifted into an FCC lattice. This explains the increasing peak stress with increasing shear. After a peak stress is reached, the stress decreases. As a larger percentage of this sample is made of grain boundary, the grains are more easily rotated, shifted, or merged. During each successive stress decrease following a peak stress, grains have combined, shifted, or merged, creating a greater percentage of FCC lattice. As the structure gains more percentage of FCC lattice, the strength increases, and another peak is reached.

5 CONCLUSION

As grain size decreases, grain boundary makes up an increasing percentage of the microstructure. As grain size goes to zero, the entire structure is made up of grain boundaries. It was proposed that grain boundary acts effectively as particles with an amorphous structure, therefore an amorphous microstructure could be considered to have a grain size of zero. Atomistic simulations up to 0.2 shear strain were first performed, showing how grain size effects yield and flow stresses in nanocrystalline copper microstructures. Then, an amorphous microstructure was simulated with the same shear strain in an effort to determine whether the amorphous sample could be considered the limiting case for the observed inverse Hall-Petch behavior.

Results from our simulations suggest that the amorphous microstructure as zero grain size is reasonable as the limiting case. For both yield and flow stress as a function of nanocrystalline grain size, the amorphous sample showed yield and flow stresses consistent with the expected inverse Hall-Petch behavior.

From our simulations, it was also observed that the 2.4 nm grain diameter nanocrystal developed increasing peak stress as the structure became increasingly composed of FCC lattice. This sample behaves somewhat like an amorphous sample, and somewhat like nanocrystalline, creating a transition in stress-strain behavior between amorphous and nanocrystalline samples with larger grain size.

6 References

1. Xiang, Q. and X.M. Guo, *The scale effect on the yield strength of nanocrystalline materials*. International Journal of Solids and Structures, 2006. **43**(25-26): p. 7793-7799.
2. Han, B.Q., E.J. Lavernia, and F.A. Mohamed, *Mechanical properties of nanostructured materials*. Reviews on Advanced Materials Science, 2005. **9**(1): p. 1-16.
3. Wolf, D., et al., *Deformation of nanocrystalline materials by molecular-dynamics simulation: relationship to experiments?* Acta Materialia, 2005. **53**(1): p. 1-40.
4. Zheng, G.P., *Grain-size effect on plastic flow in nanocrystalline cobalt by atomistic simulation*. Acta Materialia, 2007. **55**(1): p. 149-159.
5. Mishin, Y., et al., *Interatomic potentials for monoatomic metals from experimental data and ab initio calculations*. Physical Review B, 1999. **59**(5): p. 3393-3407.
6. Rapaport, D.C., *The art of molecular dynamics simulation*. 2nd ed. 2004, Cambridge, UK ; New York, NY: Cambridge University Press. xiii, 549 p.
7. Daw, M.S., S.M. Foiles, and M.I. Baskes, *The embedded-atom method: a review of theory and applications*. Material Science Reports, 1993. **9**(7-8): p. 251-310.
8. Ashcroft, N.W. and N.D. Mermin, *Solid state physics*. 1976, New York,: Holt. xxi, 826 p.
9. Mishin, Y., et al., *Structural stability and lattice defects in copper: Ab initio, tight-binding, and embedded-atom calculations*. Physical Review B, 2001. **6322**(22): p. -.
10. Boyer, R.D. and Massachusetts Institute of Technology. Dept. of Materials Science and Engineering., *Shear-induced homogeneous deformation twinning in FCC aluminum and copper via atomistic simulation*. 2003. p. 80 leaves.
11. Kumar, K.S., H. Van Swygenhoven, and S. Suresh, *Mechanical behavior of nanocrystalline metals and alloys*. Acta Materialia, 2003. **51**(19): p. 5743-5774.
12. Schiotz, J. and K.W. Jacobsen, *A maximum in the strength of nanocrystalline copper*. Science, 2003. **301**(5638): p. 1357-1359.
13. Froseth, A.G., H. Van Swygenhoven, and P.M. Derlet, *Developing realistic grain boundary networks for use in molecular dynamics simulations*. Acta Materialia, 2005. **53**(18): p. 4847-4856.
14. Lund, A.C., T.G. Nieh, and C.A. Schuh, *Tension/compression strength asymmetry in a simulated nanocrystalline metal*. Physical Review B, 2004. **69**(1): p. -.